Possible Products of the End-On Addition of N_3^- to N_5^+ and Their Stability

Stefan Fau and Rodney J. Bartlett*

Quantum Theory Project, University of Florida, Gainesville, Florida 32611-8435

Received: October 27, 2000; In Final Form: February 12, 2001

The recent synthesis of $N_5^+[AsF_6]^-$ suggests the addition of N_5^+ and N_3^- as a possible route to N_8. Because homoleptic polynitrogen compounds with more than three nitrogen atoms are nearly unknown and generally not very stable, we investigated possible products of this addition reaction. We also computed transition states for various interconversions and dissociative reactions to assess the stability of the addition products. Seven structures are minima at the B3LYP/aug-cc-PVDZ and MBPT(2)/aug-cc-pVDZ levels of theory: Five diazidyldiazenes and two diazidylaminonitrenes or N_3-N_5 complexes. Gibbs free energies based on CCSD(T)/aug-cc-pVDZ single-point calculations strongly suggest that only four of the diazidyldiazene structures are minima at higher levels of theory. We show that CCSD(T) produces good energies for molecules with some multireference character using DIP-STEOM-CCSD. In diazidyldiazenes, the loss of N_2 from one of the azidyl end groups is as likely as the loss of both azidyl groups. Isolation of covalently bonded N_8 from N_5^+ and N_3^- will be difficult because the most likely product has a decomposition barrier of only 18 kcal/mol. It may not be formed at all, because one of the approach pathways has great potential for mutual neutralization and subsequent fragmentation.

Introduction

Molecules containing only nitrogen have been one focus of research on high energy density materials (HEDM) in recent years. Proposed molecules such as octaazacubane[1−3] would release enormous amounts of energy (∼ 55 kcal/mol of N) upon decomposition into N_2 molecules. Additionally, N_2, the decomposition product, is environmentally harmless. Other, less energetic, forms of N_8[2,4] have been calculated in the last six years. For some of the N_8 molecules, barriers toward rearrangement have been investigated.[3,4] Up to now, the published work on homoleptic polynitrogen species is mostly theoretical.

In the summer of 1999, the preparation of $N_5^+[AsF_6]^-$ was published.[5] This suggests the addition of N_5^+ (**1**) and N_3^- (**2**) as an obvious route to N_8. Given the fact that N_5^+ is only the third homoleptic polynitrogen compound producable in gram quantities, we feel that a theoretical investigation of this part of the N_8 energy hypersurface might aid future attempts at synthesis of these compounds.

We explored all possible products of the end-on addition of N_3^- to N_5^+, based on the assumption that the approach and eventual bond formation between the two ions should be mainly governed by electrostatic attraction. Until the end of 1999, only one of the obvious reaction products, the linear *EEE*[6] diazidyldiazene (**4**), had been described in the literature.[4a,2d] In the summer of 2000, three more diazidyldiazene isomers had been mentioned in an article on dissociation mechanisms of known N_8 minima.[4b]

To assess the thermodynamic stability of the N_5^+ plus N_3^- addition products, we optimized a variety of transition states for rearrangement or decomposition reactions.

After describing the methods used in this work, we present some calculations on the reactants and the global minimum. These calculations show the accuracy of various methods and guide us in choosing a level for single-point calculations. In the next section, we describe the diazidyldiazene minima and discuss their stability. Then we detail the determination of electronic energies of states with some multireference character. Finally, we present our results for diazidylaminonitrene and related complexes and summarize.

Computational Details

We used the program packages Q-Chem 1.2[7] for B3LYP calculations and ACES 2[8] for MBPT(2), CCSD(T) and DIP−STEOM-CCSD[9] calculations. The aug-cc-pVDZ[10] basis set (with spherical d functions) was used as supplied by the programs. Recent work by Tobita and Bartlett[11] shows that diffuse functions are essential for the correct description of molecular symmetry of some neutral polynitrogen species. The B3LYP[12] calculations were performed using a 50 shell 302 Lebedev-point grid. Except for one benchmark calculation, the MBPT(2) and CCSD(T) calculations included the core electrons in the correlation treatment.

Geometries were fully optimized,[13] and vibrational frequency calculations or NBO[14] analyses were performed at the B3LYP and MBPT(2) levels of theory. The assignment of transition states to minima is based on geometrical similarity and "imaginary vibrations", which give the direction of the reaction coordinate at the transition state geometry. Approximate enthalpies and Gibbs free energies were calculated using the program STTHRM.[15] Improved energies were obtained by CCSD(T)//B3LYP single-point calculations. These were used with B3LYP geometry and frequency data to calculate improved enthalpies and Gibbs free energies. In cases where B3LYP and MBPT(2) structures were significantly different, CCSD(T)//MBPT(2) single-point values were determined. To judge the performance of the single-point calculations, CCSD(T) optimizations and frequency calculations using the aug-cc-pVDZ and aug-cc-pVTZ basis sets were performed for N_2, N_3^-, and N_5^+.

Heats of formation are usually determined by isodesmic

* To whom correspondence should be addressed. E-mail: fau@qtp.ufl.edu. E-mail: bartlett@qtp.ufl.edu. Fax: (352) 392-8722.

10.1021/jp003970h CCC: $20.00
Published on Web 03/29/2001

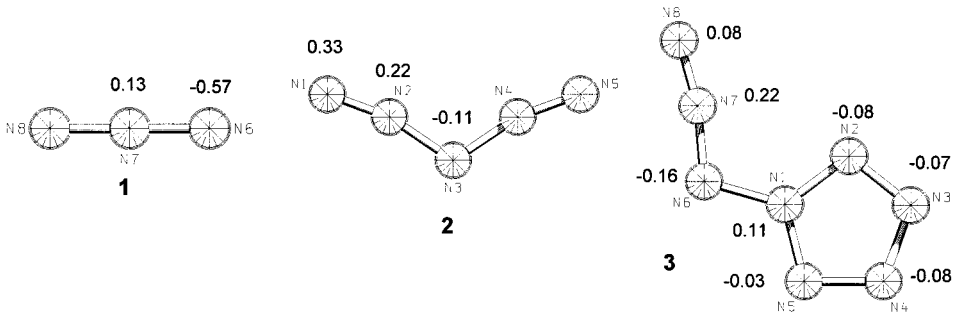

Figure 1. Structures and partial charges (NBO, B3LYP/aug-cc-pVDZ) of N_3^-, N_5^+, and **3**.

TABLE 1: Heats of Formation, Gibbs Free Energies of Formation (298.15 K, 1 bar), and Number of Imaginary Frequencies *i* for the Reactants and Azidylpentazole (3) Using the aug-cc-pVDZ Basis Set

	N_3^-, $D_{\infty h}$			N_5^+, C_{2v}			**3**, C_S		
method[a]	*i*	$\Delta_f H$	$\Delta_f G$	*i*	$\Delta_f H$	$\Delta_f G$	*i*	$\Delta_f H$	$\Delta_f G$
B3	0	34.5	39.8	0	335.9	350.1	0	195.5	226.2
M2	0	39.7	44.9	0	348.9	363.0	0	221.2	251.6
CC	0	57.2	62.5	0	354.3	368.3			
C3	0	50.1	55.4	0	349.2	363.2			
C3//B3		50.0	55.3		349.7	363.9		224.1	254.8
C3//M2		50.6	55.8		350.5	364.7		225.7	256.2
C3//B3−C3		50.9	56.3		351.1	365.4		226.4	257.2
C3//M2−C3		50.5	55.7		350.4	364.5		225.5	256.0
C3/TZ+	0	45.7	51.0						
C3/TZ+//B3		45.6	50.9		344.5	358.7			
C3/TZ+//M2		46.0	51.3		344.1	358.2			
C3/TZ+//B3−C3/TZ+		45.8	51.1		344.8	359.0			
C3/TZ+//M2−C3/TZ+		47.8	53.0		347.1	361.2			
expt[b]		48.5 ± 2.3							

[a] B3 = B3LYP, M2 = MBPT(2), CC = CCSD, C3 = CCSD(T), TZ+ = aug-cc-pVTZ. [b] Reference 20.

reactions. In this case, the design of isodesmic reactions is difficult and somewhat ambiguous because many N_8 structures show significant conjugation or unusual bond lengths. Therefore, heats of formation and Gibbs free energies of formation were calculated directly, relative to N_2. Because of the rather different bonding situation in N_2 and N_8, correlation effects have to be treated accurately to obtain good heats of formation or Gibbs free energies.

Throughout the rest of the paper, we are going to discuss CCSD(T)/aug-cc-pVDZ//B3LYP/aug-cc-pVDZ Gibbs free energies, if not specified otherwise.

Transition states involving homolytic bond breaking are usually thought to benefit from a multireference treatment like MR-CISD. When homolytic bond breaking occurs in a closed shell molecule and radical fragments are created, the multireference character of the wave function gradually increases along the reaction coordinate. In single reference CCSD, this can lead to one or more large T2-amplitudes that could be corrected by triple and quadruple excitations.

With this caveat, we report CCSD(T) energies of transition states for homolytic bond breaking. The CCSD wave functions at the transition state geometries have one T_2 amplitude of 0.2−0.4, each, exceeding the usual reliability threshold of ∼0.1. We show their reliability (in this case) by calculating the electronic energy in an indirect way. First, we calculate the electronic ground state and some excited states at the transition state geometry by DIP-STEOM-CCSD.[9] This method calculates the CCSD energy of a reference state with two electrons more than the state of interest. The energies of the state of interest and some excited states are derived by removing two electrons from the reference state in a CI-like fashion. For that reason, multireference character of the state of interest is less of a problem. The accuracy of energy differences to the reference state is estimated to be 0.16 eV.[9] Consequently, we may expect an accuracy of better than ∼0.3 eV (∼7 kcal/mol) for energy differences between the state of interest and the excited states. To get an electronic energy, we add the DIP-STEOM-CCSD energy difference to the CCSD(T) energy of a suitable excited state. This excited state has to be the lowest state of its electronic symmetry and it must be well-described by a single determinant.

Reactants and the Global Minimum

To propose addition mechanisms for N_3^- and N_5^+, we need to know their electrostatic potential or, as an approximation, their partial charges. Figure 1 shows that both terminal atoms of N_3^- have strong negative charges while the central atom is positive. In N_5^+ the terminal atoms as well as N2 and N4 are positively charged, whereas the central atom carries a negative charge. The partial charges in azidylpentazole[16] (**3**) are generally smaller but, especially in the azidyl group, still significant.

Based on the assumption of an electrostatically governed approach, N6 of N_3^- can form bonds with N1, N2, or N2 **and** N4 of N_5^+. There may be two sets of three conformers each from addition to N1, distinguished by *E* (**4**−**6**) or *Z* configuration (**7**−**9**) of the central double bond. Addition to N2 may lead to three conformers, whereas bond formation with N2 and N4 gives rise to a single conformer. The partial charge argument also points to addition of N7 to N3, but we did not find a stable molecule from that reaction. We found a singlet biradical structure of very high energy that lost an N_2 molecule during optimization. Inspection of the lowest unoccupied orbitals of N_5^+ shows three orbitals with similar energies. One has the biggest coefficients on the terminal atoms, pointing to the inside of the "V", whereas the others have big coefficients on the inside of N3 and above and below the molecular plane at the terminal atoms. Because the electrostatic argument does not favor attack

TABLE 2: Bond Lengths of 1−3 Using the aug-cc-pVDZ Basis Set

a		8−7	7−6	6−1	1−2	2−3	3−4	4−5	5−1
B3	**1**	1.190	1.190						
M2	**1**	1.222	1.222						
CC	**1**	1.194	1.194						
C3	**1**	1.206	1.206						
C3′	**1**	1.186	1.186						
expt[b]	**1**	1.188	1.188						
B3	**2**				1.119	1.308	1.308	1.119	
M2	**2**				1.144	1.315	1.315	1.144	
CC	**2**				1.121	1.338	1.338	1.121	
C3	**2**				1.131	1.339	1.339	1.131	
C3′	**2**	*c*			1.116	1.324	1.324	1.116	
B3	**3**	1.133	1.261	1.388	1.329	1.306	1.346	1.308	1.322
M2	**3**	1.151	1.280	1.390	1.336	1.338	1.347	1.337	1.331

[a] B3 = B3LYP, M2 = MBPT(2), CC = CCSD, C3 = CCSD(T), C3′ = CCSD(T)/aug-cc-pVTZ. [b] Reference 20. [c] Frozen core.

to N3, attack to N1 and bidentate out-of-plane attack to N1 and N5 seem to be most promising.

The data in Table 1 show that the experimental heat of formation of N_3^- is bracketed by the CCSD(T)/aug-cc-pVDZ and CCSD(T)/aug-cc-pVTZ values. The aug-cc-pVDZ value is 1.6 kcal/mol higher than the experimental value, whereas the aug-cc-pVTZ value is 2.8 kcal/mol lower. Therefore, we will try to give energies of CCSD(T)/aug-cc-pVDZ quality in this paper. We tested two single-point approaches to enthalpies and free energies because the N_8 structures are too big to make CCSD(T)/aug-cc-pVDZ optimizations routinely practicable. In the first approach, thermodynamic data are derived from frequencies and geometries at the B3LYP or MBPT(2) level, whereas electronic energies are determined by CCSD(T) single-point calculations. Polynitrogen species and N_2 are treated the same way. In the second approach, denoted CCSD(T)//B3LYP−CCSD(T), the treatment of the polynitrogen species is identical, but geometries and frequencies for N_2 are determined at the CCSD(T) level.

The enthalpies and free energies in CCSD(T)/aug-cc-pVDZ single-point calculations (Table 1) vary by less than 2.4 kcal/mol. The CCSD(T)/aug-cc-pVDZ//B3LYP/aug-cc-pVDZ values are closest to CCSD(T)/aug-cc-pVDZ. At the CCSD(T)/aug-cc-pVTZ level, the differences between single-point calculations are about twice as large. Here, both types of B3LYP/aug-cc-pVDZ based single-point values are very close to the CCSD-(T)/aug-cc-pVTZ reference. Because the CCSD(T)//B3LYP values seem to give the best overall results, we choose CCSD-(T)/aug-cc-pVDZ//B3LYP/aug-cc-pVDZ for our N_8 single-point calculations.

In the case of N_3^-, comparison of calculated and experimental bond lengths (Table 2) is possible. CCSD(T)/aug-cc-pVTZ and B3LYP/aug-cc-pVDZ deviate only 0.002 Å from the gas-phase data. CCSD(T)/aug-cc-pVDZ and MBPT(2)/aug-cc-pVDZ are longer by 0.018 and 0.034 Å.

Table 2 shows that MBPT(2)/aug-cc-pVDZ calculates most bonds 0.02 or 0.03 Å longer than B3LYP. The differences are greatest for bonds that are short or have a high bond order. In contrast to this trend, MBPT(2) results for **3** show nearly equal bond lengths for the pentazole ring, whereas the B3LYP bond lengths vary by 0.04 Å. At the MBPT(2) level, the pentazole ring seems to be more aromatic than at B3LYP.

A recent paper on N_2[17] shows that the experimental geometry and vibrational frequency are reproduced much better at the CCSD(T)/aug-cc-pVTZ level than at CCSD(T)/aug-cc-pVDZ. The same seems to be true for N_3^-. For N_2 and N_3^-, the difference between experimental and calculated bond distances rises as CCSD(T)/aug-cc-pVTZ ≤ B3LYP/aug-cc-pVDZ < CCSD/aug-cc-pVDZ ≤ CCSD(T)/aug-cc-pVDZ < MBPT(2)/aug-cc-pVDZ.

For N_5^+, the situation is a little different: because no experimental geometry is available, we take CCSD(T)-fc/aug-cc-pVTZ values as a reference. Both B3LYP and MBPT(2) calculate shorter N2−N3 bonds and larger N2−N3−N4 bond angles. MBPT(2) is better with these parameters, but it calculates the N1−N2 triple bond 0.03 Å longer than the reference, whereas B3LYP is nearly on the spot. CCSD comes closest to the reference values (Table 3).

A comparison of the bond angles at different levels of theory shows that B3LYP and MBPT(2) differ by up to 2.5° although the difference is usually below 1°. In N_5^+, CCSD comes closest to the CCSD(T)-fc/aug-cc-pVTZ reference. CCSD(T)/aug-cc-pVDZ, MBPT(2), and B3LYP differ increasingly more.

Products of Addition to N1

There are two sets of isomers, distinguished by the *E* (**4**−**6**) or *Z* configuration (**7**) of the N1−N2 double bond. The conformers are characterized by the *E* or *Z* configuration[6] of the adjacent single bonds (see Figure 2). The Gibbs free energies (Table 4) with respect to azidylpentazole[4,2d] (**3**) range between 13 and 17 kcal/mol. The *xEx* conformers **4**−**6** differ in free energy by about 2 kcal/mol. Although the *gZE* and *ZZE* structures (**8a**,**b**) are (shallow) minima at B3LYP and MBPT-(2), respectively, single-point calculations indicate that **8b** is a transition state at the CCSD(T) level: the CCSD(T)//B3LYP electronic energies fall monotonically from **8b** over **8a** and **7**−**8** to **7**. The *ZZZ* conformer does not exist. The closest approximation, *gZg* diazidyldiazene **8**−**8′**, is a transition state for the degenerate rearrangement of *gZE* (**8a**) to *EZg* (**8a′**) diazidyldiazene.

We also calculated two transition states for rotation around the N6−N1 bond. In **4**−**5**, the barrier to rotation ($\Delta_a G_{298}$°) is lower than 6.5 kcal/mol, allowing reaction at room temperature. We expect a second transition state, **5**−**6**, to exist with a similar barrier. Furthermore, **7**−**8** transforms **8a** (or the MBPT(2) minimum **8b**) into **7** with a barrier of 1 kcal/mol. As mentioned above, at the CCSD(T)/aug-cc-pVDZ level of theory, only **8b** might be a stationary point (a transition state).

According to chemical intuition, addition of N_3^- to the terminal atom of N_5^+ should produce diazidyldiazene with an *E* configuration of the central double bond. Therefore, **7** is

TABLE 3: Bond Angles of 2 and 3 Using the aug-cc-pVDZ Basis Set

a		8−7−6	7−6−1	6−1−2	1−2−3	2−3−4	3−4−5	4−5−1	5−1−2
B3	**2**				166.0	111.9	166.0		
M2	**2**				167.2	110.2	167.2		
CC	**2**				167.1	107.7	167.1		
C3	**2**				166.0	108.0	166.0		
C3′	**2**				167.1	108.5	167.1		
B3	**3**	169.4	111.1	126.7	103.9	109.3	109.5	103.9	113.3
M2	**3**	169.7	108.7	125.7	103.1	109.4	109.9	103.0	114.7

[a] B3 = B3LYP, M2 = MBPT(2), CC = CCSD, C3 = CCSD(T), C3′ = CCSD(T)-fc/aug-cc-pVTZ.

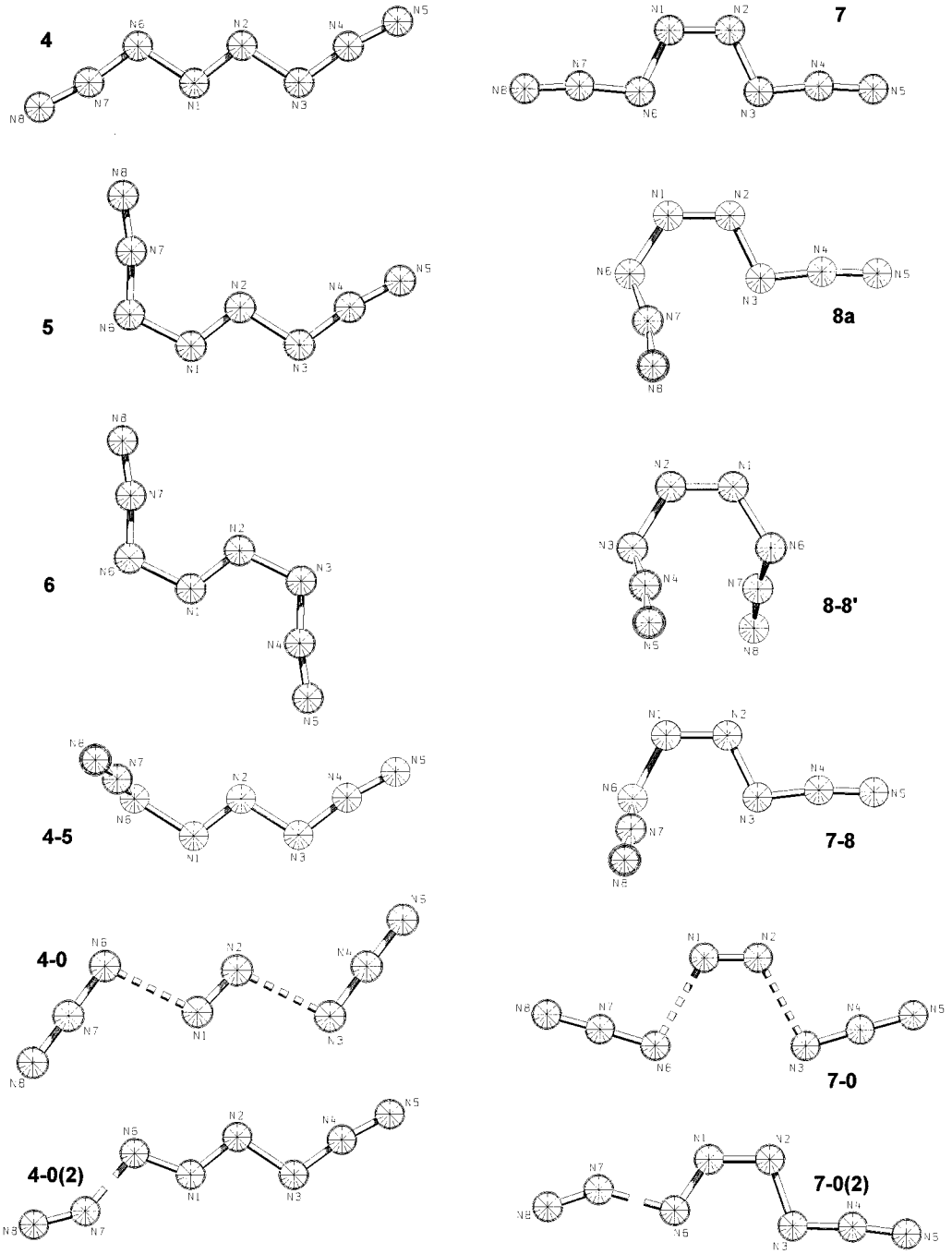

Figure 2. Structures (B3LYP/aug-cc-pVDZ) of diazidyldiazenes and transition states.

accessible by inversion of the N6−N1−N2 angle in **5** or rotation of the azidyl group around the N1−N2 double bond in **4**. Because breaking a NN double bond should be much less for favorable than inverting the N6−N1−N2 angle, we searched the inversion transition state only. In a series of partial optimizations with constraint on the N6−N1−N2 angle, **5** lost N_2 before N6−N1−N2 came close to 180°. It seems like *E*-diazidyldiazenes cannot be converted directly into *Z*-diazidyldiazenes.

To judge the stability of diazidyldiazenes, we optimized two transition states, **4**−**0** and **7**−**0**. They feature simultaneous breaking of the longest and weakest bonds in **4** and **7**, the N2−N3 and N1−N6 bonds. These bonds are the weakest by the empirical bond length ↔ bond strength correlation, the force constants, and the overlap weighted NAO bond orders. The simultaneous bond breaking is presumably due to an instability of the $N_5^{\bullet}$ radical, causing its dissociation into N_2 and $N_3^{\bullet}$. At CCSD(T)/aug-cc-pVDZ//MBPT(2)/aug-cc-pVDZ, the dissociation reaction of **4** has a barrier of 18 kcal/mol; for **7**, $\Delta_a G_{298}°$ is 15 kcal/mol. These transition states have some multireference character, but the CCSD(T) energies are (in this case) reliable as will be shown later.

Another dissociation mechanism, without open-shell problems at the TS, has recently been described.[4b] Here an azidyl endgroup loses N_2 and leaves N_6. To compute Gibbs free energies we re-optimized **4**−**0(2)** and **7**−**0(2)**. We found that they have not C_1 but C_S symmetry at the B3LYP/aug-cc-pVDZ level. The Gibbs free energies of activation are 19 and 16 kcal/mol, very similar to the barriers for loosing both azidyl groups (Figure 3).

A comparison of the data in Table 4 shows that the Gibbs free energies at the B3LYP level are 2−4 kcal/mol lower than

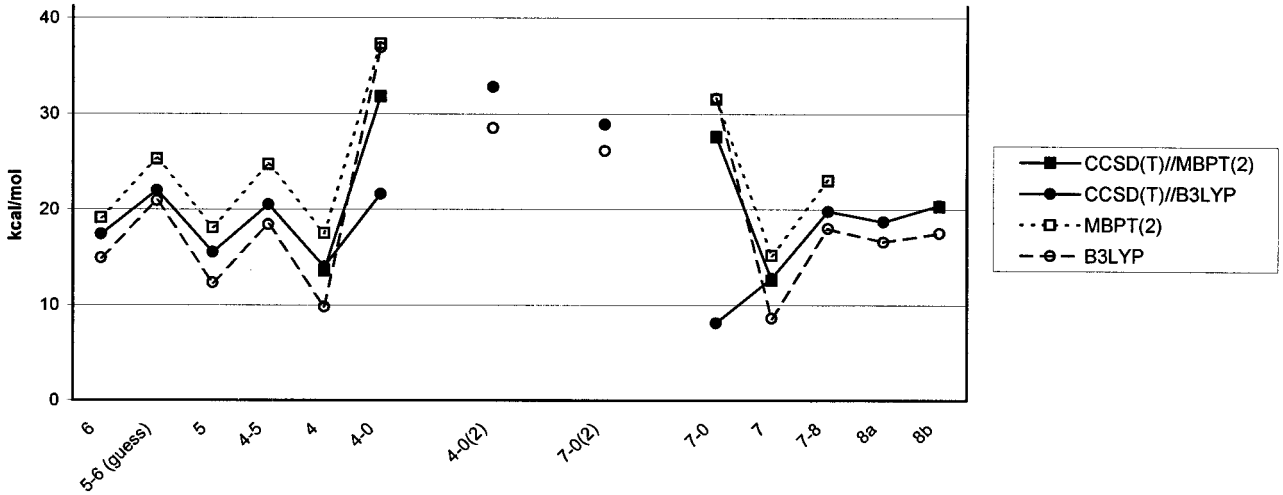

Figure 3. Gibbs free energies of diazidyldiazenes relative to azidylpentazole **3**.

TABLE 4: Diazidyldiazenes and Transition States, Number of Imaginary Frequencies *i*, Enthalpies, and Gibbs Free Energies (298.15 K, 1 bar) Relative to Azidylpentazole 3 at B3LYP/aug-cc-pVDZ, MBPT(2)/aug-cc-pVDZ and CCSD or CCSD(T)/aug-cc-pVDZ//B3LYP/aug-cc-pVDZ[a]

		B3LYP			MBPT(2)			CCSD// B3LYP		CCSD(T)// B3LYP	
	sym	*i*	Δ*H*	Δ*G*	*i*	Δ*H*	Δ*G*	Δ*H*	Δ*G*	Δ*H*	Δ*G*
4a	C_{2h}	0	10.6	9.8				14.6	13.9	14.7	14.0
4b	C_{2h}				0	18.2	17.5	14.2[b]	13.6[b]	14.3[b]	13.6[b]
5	C_S	0	13.7	12.3	0	19.2	18.1	17.3	15.9	16.9	15.5
6	C_{2h}	0	16.0	14.9	0	19.8	19.1	19.1	18.1	18.5	17.4
7a	C_{2v}	0	9.5	8.6				14.6	13.7	13.7	12.8
7b	C_{2v}				0	15.9	15.2	14.3[b]	13.6[b]	13.3[b]	12.6[b]
8a	C_1	0	18.3	16.6		*c*		21.9	20.2	20.4	18.7
8b	C_S	1	17.8	17.5	0	22.1	20.3	22.5	22.1	20.7	20.4
4−5	C_1	1	18.9	18.4	1	24.9	24.7	21.0	20.6	20.9	20.5
7−8	C_1	1	18.2	18.0	1	22.9	23.0	21.3	21.1	20.0	19.8
8−8′	C_2	1	28.5	28.3							
5−7	C_S		*d*								
4−0a	C_{2h}	1	39.4	36.9				48.8	46.3	24.1	21.6
4−0b	C_{2h}				1	41.2	37.3	47.2[b]	43.3[b]	35.7[b]	31.8[b]
7−0a	C_{2v}	1	36.1	31.6				43.6	39.1	12.6	8.1
7−0b	C_{2v}				1	34.6	31.5	43.4[b]	40.3[b]	30.7[b]	27.6[b]
4−0(2)	C_S	1	30.2	28.5				34.4	32.8	34.5	32.8
7−0(2)	C_S	1	27.9	26.1				31.2	29.3	30.8	28.9

[a] CCSD or CCSD(T) electronic energies with B3LYP geometry and vibrational data. [b] CCSD or CCSD(T) electronic energies with MBPT(2) geometry and vibrational data. [c] Optimized to C_S at MBPT(2). [d] Dissociates before N2−N1−N6 reaches 180°.

the CCSD(T) values. The MBPT(2) values are 2−4 kcal/mol higher than the CCSD(T) values. The CCSD values are less than 2 kcal/mol higher. This comparison excludes the transition states for homolytic bond breaking, **4−0** and **7−0**. In their case, MBPT(2) values are 5 kcal/mol higher than CCSD(T), whereas the B3LYP values are about 20 kcal/mol too high. The CCSD energies are 12−28 kcal/mol too high, depending on which geometries are used. For the minima **4** and **7**, choosing B3LYP or MBPT(2) geometries makes little difference.

Looking directly at the Gibbs free energies of activation (Table 5), all methods of computation give good results for rotations and heterolytic bond breaking. B3LYP has the biggest average deviation from the CCSD(T) barriers with +2.3 kcal/mol. For the homolytic bond breaking, only MBPT(2) comes close to the CCSD(T) values. The other methods overestimate the barriers by about 8−14 kcal/mol.

The B3LYP bond lengths (Table 6a) of **4−8** show a common pattern for all of the conformers. The terminal N8−N7 and N4−N5 bonds are a bit shorter than the terminal NN bond in H_3C-N_3 (1.143 Å), whereas the N7−N6 and N3−N4 bonds are slightly longer than the inner NN bond of H_3C-N_3 (1.236 Å). This indicates a slightly stronger localization of the terminal π

TABLE 5: Gibbs Free Energies of Activation at 298 K and 1 bar in kcal/mol.

	B3LYP	MBPT(2)	CCSD//	CCSD(T)//
4 → 4−5	8.6	7.2	6.7	6.5
7 → 7−8	9.4	7.8	7.4	7.0
4 → 4−0	27.1	19.8	29.7[a]	18.2[a]
7 → 7−0	23.0	16.3	26.7[a]	15.0[a]
4 → 4−0(2)	18.7		18.9	18.8
7 → 7−0(2)	17.5		15.6	16.1

[a] MBPT(2) geometry and vibrational data. Barriers for the B3LYP geometries are about the same at CCSD and much lower (+7.6 and −4.7 kcal/mol) at CCSD(T).

TABLE 6: Diazidyldiazenes and Transition States

(A) Bond Lengths in Å at B3LYP/aug-cc-pVDZ

	8−7	7−6	6−1	1−2	2−3	3−4	4−5
4	1.135	1.259	1.396	1.251	1.396	1.259	1.135
5	1.133	1.274	1.387	1.253	1.399	1.258	1.135
6	1.133	1.272	1.390	1.255	1.390	1.272	1.133
7	1.135	1.257	1.416	1.242	1.416	1.257	1.135
8a[a]	1.136	1.261	1.417	1.243	1.421	1.256	1.134
8b	1.134	1.280	1.378	1.248	1.425	1.252	1.135
8−8′[b]	1.138	1.256	1.451	1.235	1.451	1.256	1.138
4−5[c]	1.140	1.247	1.452	1.243	1.398	1.264	1.132
7−8[d]	1.140	1.246	1.467	1.236	1.413	1.262	1.132
4−0	1.158	1.217	2.031	1.133	2.031	1.217	1.158
7−0	1.163	1.210	2.116	1.123	2.116	1.210	1.163
4−0(2)	1.117	1.605	1.265	1.262	1.427	1.249	1.140
7−0(2)	1.115	1.629	1.272	1.257	1.459	1.246	1.139

(B) Bond Lengths in Å at MBPT(2)/aug-cc-pVDZ

	8−7	7−6	6−1	1−2	2−3	3−4	4−5
4	1.154	1.275	1.406	1.273	1.406	1.275	1.154
5	1.157	1.282	1.397	1.278	1.406	1.275	1.154
6	1.157	1.283	1.395	1.284	1.395	1.283	1.157
7	1.155	1.272	1.420	1.265	1.420	1.272	1.155
8b	1.164	1.287	1.379	1.274	1.423	1.267	1.155
4−5[e]	1.158	1.265	1.467	1.267	1.403	1.278	1.153
7−8[f]	1.160	1.260	1.482	1.259	1.411	1.278	1.154
4−0	1.169	1.255	1.876	1.168	1.876	1.255	1.169
7−0	1.170	1.252	1.862	1.159	1.862	1.252	1.170

[a] 2−1−6−7 = 42.3°. [b] 2−1−6−7 = 57.3°. [c] 2−1−6−7 = 83.5°. [d] 2−1−6−7 = 79.2°. [e] 2−1−6−7 = 85.1°. [f] 2−1−6−7 = 91.4°.

TABLE 7: Diazidyldiazenes and Transition States

(A) Bond Angles in Degrees at B3LYP/aug-cc-pVDZ

	sym	8−7−6	7−6−1	6−1−2	1−2−3	2−3−4	3−4−5
4	C_{2h}	170.4	109.9	108.2	108.2	109.9	170.4
5	C_S	170.2	115.8	114.3	108.9	110.1	170.7
6	C_{2h}	170.4	115.5	114.9	114.9	115.5	170.4
7	C_{2v}	171.5	109.9	115.4	115.4	109.9	171.5
8a	C_1	168.5	118.2	123.0	116.1	109.9	172.5
8−8′	C_2	171.7	113.9	121.7	121.7	113.9	171.7
8−8′	C_S	162.8	123.2	126.8	115.8	110.4	173.1
4−5	C_1	170.2	109.5	109.0	109.1	111.9	173.0
7−8	C_1	171.3	109.4	116.3	117.5	112.7	173.4
4−0	C_{2h}	178.9	99.6	107.0	107.0	99.6	178.9
7−0	C_{2v}	178.7	102.2	118.8	118.8	102.2	178.7
4−0(2)	C_S	145.1	109.6	120.3	107.1	109.9	172.0
7−0(2)	C_S	146.0	108.6	123.9	109.6	110.3	173.7

(B) Bond Angles in Degrees at MBPT(2)/aug-cc-pVDZ

	sym	8−7−6	7−6−1	6−1−2	1−2−3	2−3−4	3−4−5
4	C_{2h}	170.3	108.0	106.9	106.9	108.0	170.3
5	C_S	170.8	114.1	112.5	107.7	108.0	170.6
6	C_{2h}	170.7	113.7	113.4	113.4	113.7	170.7
7	C_{2v}	170.6	108.4	113.7	113.7	108.4	170.6
8b	C_S	161.7	123.7	124.5	114.1	109.3	171.9
4−5	C_1	172.9	108.7	107.1	107.7	107.7	170.2
7−8	C_1	173.2	109.2	114.1	114.7	108.0	170.1
4−0	C_{2h}	176.8	97.3	103.9	103.9	97.3	176.8
7−0	C_{2v}	175.7	101.6	116.4	116.4	101.6	175.7

bonds. The N1−N2 bond is slightly longer than the NN double bond in *trans*-$H_3CN{=}NCH_3$ (1.240 Å). Finally, the N6−N1 and N2−N3 bonds are significantly shorter than the N−N single bond in C_{2h} $(H_3C)_2N{-}N(CH_3)_2$ (1.481 Å). This may be attributed to a weak π bond, because of delocalization of the N3 and N6 π lone pairs into the N1−N2 π antibond. At the MBPT(2) level (Table 6b), the bonds are up to 0.03 Å longer, showing a bigger increase in bond length with higher bond order (Table 7).

Comparing the structures shows that the N1−N2, *Z* conformers have shorter N1−N2 bonds (0.01 Å), longer N6−N1 and N2−N3 bonds (0.02 Å), and larger bond angles N6−N1−N2 and N1−N2−N3 than the *E* conformers. *Z* conformations at the N6−N1 or N2−N3 bonds are accompanied by longer N7−N6 or N3−N4 bonds (0.01 Å) and a similar increase of adjacent bond angles.

The transition states **8−8′**, **4−5**, and **7−8** show a clear increase in N1−N6 bond length and a slight equilibration of the N6−N7 and N7−N8 bond lengths. This can be attributed to the loss of bonding π interactions across the N1−N6 bond and reorganization in the N6, N7, and N8 azidyl group. The transition states **4−0** and **7−0** have nearly broken N6−N1 and N2−N3 bonds. At B3LYP, these bonds are ∼0.2 Å longer than at MBPT(2). Both transition states show strong equilibration of the bonds in the azidyl groups. Finally, **4−0 (2)** and **7−0 (2)** lead to N_6 and N_2. The N6−N7 bonds are only 0.12 and 0.14 Å longer than in C_{2h} $(H_3C)_2N{-}N(CH_3)_2$, indicating very early transition states.

The electronic structures of **3−8**, described in terms of natural localized molecular orbitals (NLMOs, see the Supporting Information), are as similar as their bond lengths. There aretwo triple bonds (N8−N7 and N4−N5), an N1−N2 double bond, and two π lone pairs at N6 and N3. Each π lone pair is strongly delocalized: ∼20% into the terminal π antibond and 7% into the N1−N2 π antibond. There is a σ lone pair at every atom except N7 and N4. The σ bonds to N7 and N4 are somewhat polar (∼ 57% of the bonding electron pair at N4/N7 and 43% at the other atom). The other σ bonds are nonpolar. In the nonplanar structures, the π interactions are interrupted at the twisted bonds.

TABLE 8: Diazidyldiazenes and Transition States, Natural Atomic Charges in e⁻ at B3LYP/aug-cc-pVDZ

	sym	N8	N7	N6	N1	N2	N3	N4	N5
4	C_{2h}	0.03	0.23	−0.20	−0.06	−0.06	−0.20	0.23	0.03
5	C_S	0.05	0.22	−0.20	−0.02	−0.12	−0.19	0.23	0.03
6	C_{2h}	0.05	0.22	−0.20	−0.08	−0.08	−0.20	0.22	0.05
7	C_{2v}	0.03	0.23	−0.23	−0.03	−0.03	−0.23	0.23	0.03
8a	C_1	0.02	0.21	−0.22	0.00	−0.03	−0.27	0.24	0.04
8−8′	C_S	0.04	0.21	−0.21	0.00	−0.05	−0.27	0.24	0.03
8−8′	C_2	0.02	0.20	−0.24	0.02	0.02	−0.24	0.20	0.02
4−5	C_1	−0.01	0.21	−0.22	−0.03	−0.04	−0.20	0.23	0.05
7−8	C_1	−0.02	0.21	−0.23	0.00	0.00	−0.24	0.24	0.05
4−0	C_{2h}	−0.02	0.15	−0.15	0.03	0.03	−0.15	0.15	−0.02
7−0	C_{2v}	−0.03	0.13	−0.13	0.04	0.04	−0.13	0.13	−0.03
4−0(2)	C_S	0.13	0.11	−0.08	−0.00	−0.15	−0.21	0.22	−0.01
7−0(2)	C_S	0.13	0.12	−0.10	0.01	−0.12	−0.26	0.23	−0.01

The partial charges (natural charges; Table 8) are quite large for a homoleptic neutral molecule: ∼0.23 at N7/N4 and −0.20 to −0.27 at N6/N3. The other atoms are only slightly charged. These partial charges have the same pattern as the formal charges used in the Lewis structure derived from the NLMOs. Despite the considerable atomic charges, the azidyl end groups carry only a small charge. It is slightly positive in the planar structures and becomes slightly negative when the azidyl group is rotated out of the molecular plane.

The covalent (overlap-weighted NAO) bond orders (see the Supporting Information) show a pattern similar to the NLMOs: they are highest for the triple bonds (∼1.67), lower for the central double bond (∼1.24), and lowest for the N6−N1 and N2−N3 σ bonds (∼ 0.88). The covalent bond order of the N7−N6 and N3−N4 bonds is higher (∼ 1.20), because of strong delocalization of both π lone pairs. Compared to the reference molecule[18] $H_3C{-}N_3$, the terminal bonds of the azidyl group are a little stronger, whereas the inner bonds are a little weaker. The N1−N2 double bond is weaker than the double bond in *trans*-$H_3C{-}N{=}N{-}CH_3$, too, whereas the N1−N6 and N2−N3 single bonds are stronger than the N−N bond in $(H_3C)_2N{-}N(CH_3)_2$.

Calculating Reliable Energies for States with Some Multireference Character

Some of the transition states in this work describe homolytic bond breaking. In the case of closed shell singlet states, the products are open shells, and the multireference character gradually increases during the reaction. This is illustrated by the data in Table 9 (the breaking bonds are longer in **7−0a** than in **7−0b**). The MBPT(2) and CCSD(T) energies of activation become smaller with increasing multireference character, whereas the CCSD energy of activation remains virtually unchanged. This may be interpreted as a consequence of the perturbation not being small anymore so that MBPT(2) and the perturbative triples correction in CCSD(T) become unreliable.

TABLE 9: Largest T_2 Amplitudes, RHF Orbital Energy Differences $\Delta\epsilon$ in eV, and Electronic Energies of Activation in kcal/mol

	7−0b			**7−0a**		
	$\Delta\epsilon$	max T_2	$\Delta_a E$	$\Delta\epsilon$	max T_2	$\Delta_a E$
MBPT(2)	8.1	−0.13	21.0	4.5	−0.38	6.7
CCSD	8.1	−0.18	31.4	4.5	−0.39	31.4
CCSD(T)	8.1	−0.18	19.7	4.5	−0.39	1.4

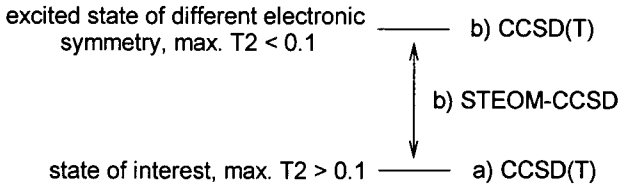

Figure 4. Two ways to calculate the electronic energy of a state with some multireference character.

TABLE 10: Ground and Relevant Excited States of 4−0, 7−0, 10−0, and 11−0, Determined by DIP-STEOM-CCSD/aug-cc-pVDZ at the B3LYP/aug-cc-pVDZ and MBPT(2)/aug-cc-pVDZ Optimized Geometries[a]

	state	% active[b]	el. en.	electrons removed from[c]	ΔE
4−0a	^1A_g	99.98	−436.717 74	36.1% −1[A_g], −1[A_g]	0.0
				63.2% −1[B_u], −1[B_u]	
	^3B_u	99.98	−436.712 46	98.1% −1[A_g], −1[B_u]	5.3
4−0b	^1A_g	99.93	−436.686 18	17.4% −1[A_g], −1[A_g]	0.0
				81.7% −1[B_u], −1[B_u]	
	^3B_u	99.95	−436.657 23	96.8% −1[A_g], −1[B_u]	29.0
				2.8% −1[A_g], −2[B_u]	
7−0a	$^1A_1$	100.00	−436.735 10	40.9% −1[B_2], −1[B_2]	0.0
				58.7% −1[A_1], −1[A_1]	
	$^3B_2$	99.99	−436.732 78	99.1% −1[A_1], −1[B_2]	2.3
7−0b	$^1A_1$	99.94	−436.694 59	19.3% −1[B_2], −1[B_2]	0.0
				80.0% −1[A_1], −1[A_1]	
	$^3B_2$	99.92	−436.670 93	97.7% −1[A_1], −1[B_2]	23.7
10−0	$^1A'$	99.89	−436.712 96	67.9% −1[A′], −1[A′]	0.0
				7.1% −1[A′], −2[A′]	
				24.7% −2[A′], −2[A′]	
	$^3A'$	99.91	−436.704 27	99.7% −1[A′], −2[A′]	8.7
11−0	$^1A_1$	99.98	−436.718 93	33.3% −1[B_2], −1[B_2]	0.0
				66.4% −1[A_1], −1[A_1]	
	$^3B_2$	99.99	−436.712 97	99.5% −1[A_1], −1[B_2]	6.0

[a] The energy is given in hartree, ΔE in mhartree. The extra electrons in the DIP reference occupy orbitals of Bu, A1, A′, and A1 symmetry. The HOMO − 1 orbitals (HOMO of the neutral species) are of Ag, B2, A′, and B2 symmetry. [b] Percentage of the DIP vector consisting of IP-EOM-CCSD vectors included in the similarity transformation. It should be bigger than ca. 95%. [c] Contributions greater than 2.5%. The notation $-n[L]$ means the n-highest occupied orbital of irrep L, whereas $n[L]$ indicates the n-lowest unoccupied orbital of irrep L.

To provide reliable energies for states with multireference character, we used a different approach (b in Figure 4). First, we used DIP-STEOM-CCSD to calculate the energies of the lowest singlets and triplets of each symmetry that are describable by removing two electrons from a double anion reference state. In all double anions, the two extra electrons occupied what had been the LUMO of the neutral molecule. The biggest CCSD T_2 amplitudes in these double anion states were smaller than 0.06, showing that these reference states are well described. Then we looked at the description of the states that are derived by removing two electrons from the reference in a CI-like fashion. These are the ground state and some of the excited states of N_8 in the transition state geometry determined at the B3LYP or MBPT(2) level. In Table 10, we see that the singlet ground states have moderate to strong multireference character. The triplet excited states seem to be single-reference states. The IP-EOM-CC vectors used to describe these states have no double excitation coefficients bigger than 0.05. None of the IP-EOM-CC vectors used in the similarity transformation has less than 80% single excitation character. Excited states of other symmetries have been calculated, too, but are not presented here because they have strong multireference character and are not suitable for CCSD or CCSD(T) calculations. In the third step, we calculated UHF based CCSD(T)/aug-cc-pVDZ energies for the triplet states. All T_2 amplitudes are smaller than 0.06, so CCSD(T) should give good results. Finally, we combine the CCSD(T) energies of the triplet states with the DIP-STEOM-CCSD energy difference between singlet and triplet states to get approximate energies for the singlets with some multireference character. These values are shown in Table 11. The difference between energies calculated by the DIP-STEOM route and energies calculated by UHF-based CCSD(T) for the singlet states is 3 mhartree (∼2 kcal/mol) or less. This agreement is seen for all six geometries, leading us to believe that the error in the DIP-STEOM-CCSD energy differences is smaller than the expected maximum of 7 kcal/mol.

The agreement between the DIP-STEOM-CCSD and CCSD descriptions of the multireference singlets (Table 12) is also good: the dominant contributions agree to better than 2% for the MBPT(2) structures and better than 4% for the B3LYP structures. The difference between DIP-STEOM-CCSD derived energies and CCSD energies for the multireference singlet states is much larger: about 12 kcal/mol for the MBPT(2) structures and 29−35 kcal/mol for the B3LYP structures, where CCSD has significantly larger T_2 amplitudes. This shows that CCSD energies may become questionable when the largest T_2 amplitudes exceed 0.1; that inclusion of higher excitation clusters corrects this misbehavior and that (at least in these cases) perturbative triple excitations are sufficient to solve the problem.

To confirm that our conclusions on the single-reference

TABLE 11: Energies (in hartree) of the Singlet Ground States Calculated Directly or Derived from Excited State Calculations and DIP-STEOM-CCSD Energy Differences[a]

							energy−ΔE(DIP)	
	state	ref	max T_2	"excitation" from	to	ΔE(DIP)	CCSD	CCSD(T)
4−0a	^1A_g	RHF	0.33	−1[A_g] −1[A_g]	1[B_u] 1[B_u]		−436.6877	−436.8014
	^3B_u	UHF	0.05			0.0053	−436.7358	−436.8041
	^3B_u	QRHF	0.07			0.0053	−436.7340	−436.8028
4−0b	^1A_g	RHF	0.18	−1[A_g] −1[A_g]	1[B_u] 1[B_u]		−436.6895	−436.7849
	^3B_u	UHF	0.06			0.0290	−436.7067	−436.7819
7−0a	$^1A_1$	RHF	0.39	−1[B_2] −1[B_2]	1[A_1] 1[A_1]		−436.6970	−436.8207
	$^3B_2$	UHF	0.04			0.0023	−436.7543	−436.8212
	$^3B_2$	QRHF	0.05			0.0023	−436.7526	−436.8194
7−0b	$^1A_1$	RHF	0.18	−1[B_2] −1[B_2]	1[A_1] 1[A_1]		−436.6959	−436.7933
	$^3B_2$	UHF	0.05			0.0237	−436.7157	−436.7904
10−0	1A′	RHF	0.26	−1[A′] −1[A′]	1[A′] 1[A′]		−436.6958	−436.7993
	3A′	UHF	0.04			0.0087	−436.7319	−436.8002
11−0	$^1A_1$	RHF	0.31	−1[B_2] −1[B_2]	1[A_1] 1[A_1]		−436.6924	−436.8033
	$^3B_2$	UHF	0.04			0.0060	−436.7382	−436.8058

[a] Very large T_2 amplitudes are characterized. [b] The notation $-n[L]$ means the n-highest occupied orbital of irrep L, whereas $n[L]$ indicates the n-lowest unoccupied orbital of irrep L.

TABLE 12: Distribution of the Electrons onto the HOMO and LUMO of the Neutral Closed Shell Reference State as Derived from the Dominant Contributions of the CCSD T_2 Amplitudes or the DIP-STEOM Description of the Singlet State

	DIP-STEOM-CCSD		CCSD	
	HOMO	LUMO	HOMO	LUMO
4−0a	64% A_g	37% B_u	67% A_g	33% B_u
4−0b	83% A_g	17% B_u	82% A_g	18% B_u
7−0a	59% B_2	41% A_1	61% B_2	39% A_1
7−0b	81% B_2	20% A_1	82% B_2	18% A_1
10−0	75% A′	32% A′	74% A′	26% A′
11−0	67% B_2	34% A_1	69% B_2	31% A_1

character of the triplets are not tainted by significant differences between the occupied orbitals that the neutral and dianionic references have in common, we also calculated two of the triplet states based on QRHF. We removed two electrons from the two orbitals of the dianionic reference state that dominate the DIP-STEOM description of the triplet state before conducting the CCSD part of the calculation. The resulting energies (Table 11) are only slightly higher than the UHF-based energies, as are the largest T_2 amplitudes. This shows that the QRHF reference is nearly as good as the UHF reference and, in conclusion, that the occupied orbitals of the dianionic reference correspond well to those of the neutral reference.

Products of Addition to N2 or to N2 and N4

At the B3LYP or MBPT(2) level, this reaction gives rise to the loosely bound N_3-N_5 complexes **10** and **11b** (Figure 5). Complex **11a** is of the aminonitrene structure type that was previously reported not to be a minimum.[4] In **10** and **11b**, the azidyl group coordinates to N2 of a distorted N_5 unit. Complex

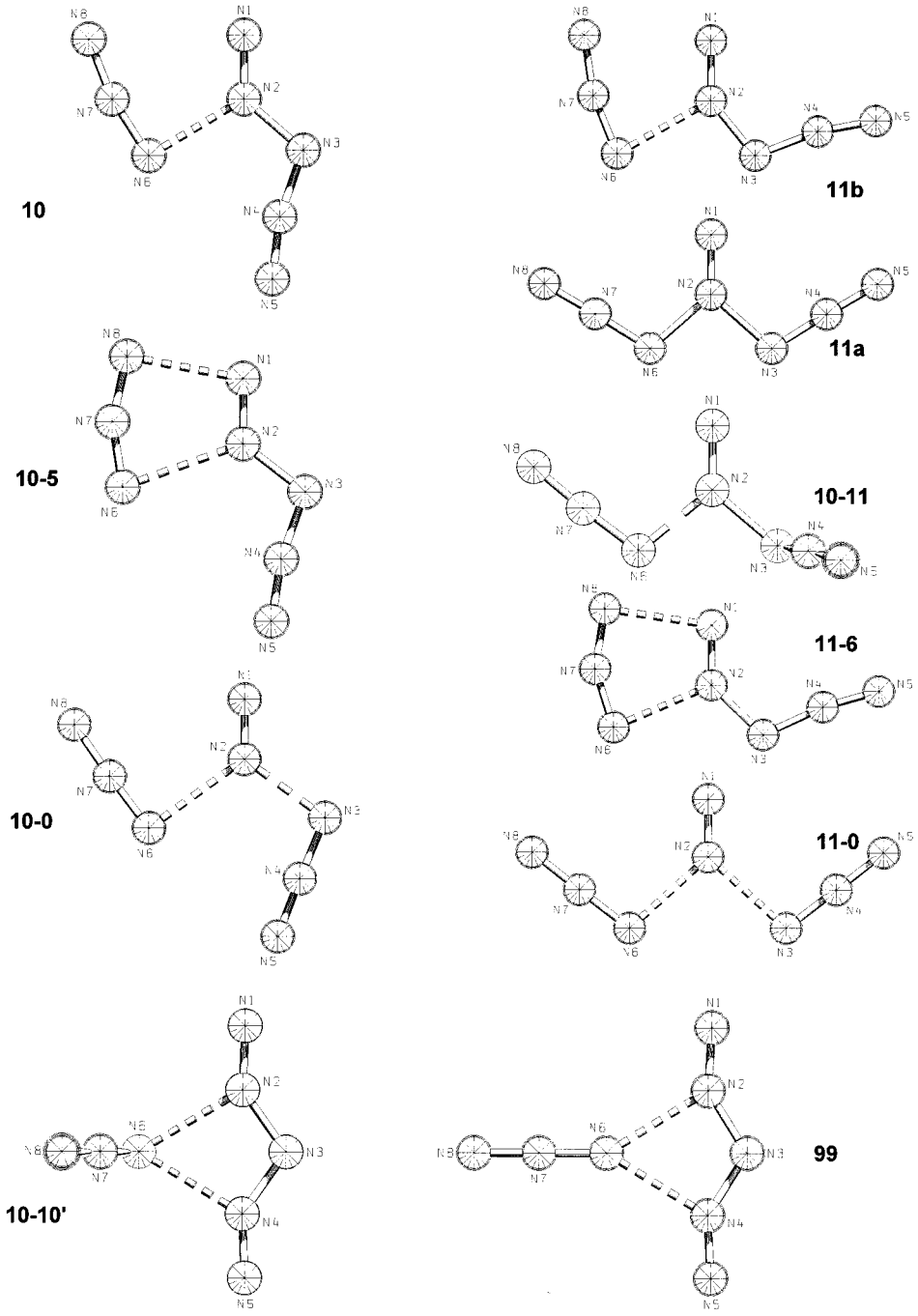

Figure 5. Structures (B3LYP/aug-cc-pVDZ) of branched N_8.

TABLE 13: Enthalpies and Gibbs Free Energies (298.15 K, 1 bar) Relative to Azidylpentazole (3) and Number of Imaginary Frequencies *i* at B3LYP/aug-cc-pVDZ, MBPT(2)/aug-cc-pVDZ, and CCSD or CCSD(T)/cc-pVDZ//B3LYP/aug-cc-pVDZ[a]

		B3LYP			MBPT(2)			CCSD//B3LYP		CCSD(T)//B3LYP	
	sym	*i*	ΔH	ΔG	*i*	ΔH	ΔG	ΔH	ΔG	ΔH	ΔG
10	C_S	0	31.9	29.7	0	19.0	17.5	43.3	41.0	36.5	34.2
11a	C_{2v}	0	34.4	32.0		dissociated		41.1	38.8	37.9	35.6
11b	C_S		*b*		0	29.0	26.9	55.3[c]	53.2[c]	46.4[c]	44.3[c]
10−5	C_S	1	32.5	31.7				38.5	37.7	31.3	30.5
10−0	C_S	1	36.4	32.1				44.8	40.5	26.4	22.1
								22.1[d]	17.8[d]	25.8[d]	21.5[d]
10−11	C_1	1	37.2	35.8	1	33.3	32.8	43.5	42.1	38.9	37.5
11−6	C_S	1	38.3	37.2	1	35.6	34.8	43.9	42.8	36.6	35.5
11−0	C_{2v}	1	38.3	34.4				46.7	42.9	23.7	19.9
								17.8[e]	14.0[e]	22.0[e]	18.2[e]
10−10′	C_S	1	39.3	37.9				50.4	49.0	42.4	41.0
99	C_{2v}	2	45.3	45.6	2	34.3	35.3	57.1	57.4	50.4	50.6

[a] CCSD or CCSD(T) energies with B3LYP geometry and vibrational data. [b] C_S optimized to C_{2v} at B3LYP. [c] MBPT(2) geometry and vibrational data, max $T_2 = -0.13$, direct comparison of CCSD(T) electronic energies shows **11b** is 7.3 kcal/mol higher in electronic energy than **11a**. [d] Using the electronic energies derived from the $^3A'$ state in Table 12. [e] Using the electronic energies derived from the $^3B_2$ state in Table 12.

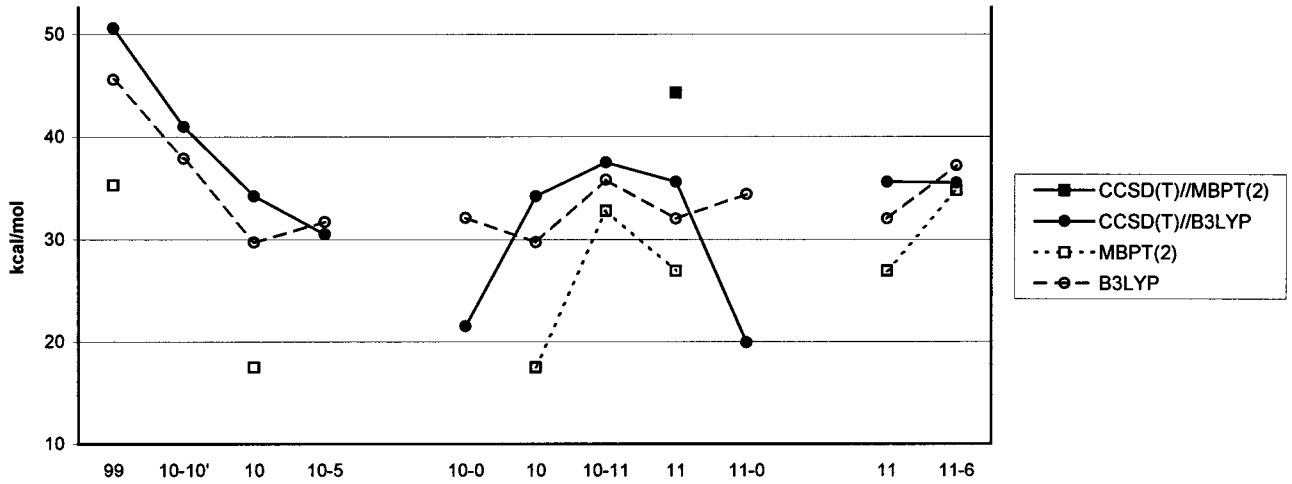

Figure 6. Gibbs free energies of diazidylaminonitrene and related complexes relative to azidylpentazole **3**.

11a is the symmetric version of **11b** with elongated bonds to the azidyl groups. CCSD(T) single-point calculations show that **11b** is 7 kcal/mol higher in electronic energy than **11a**.

As will be shown in the following paragraphs, **10**, **11a**, and **11b** are shallow minima at the B3LYP and MBPT(2) levels only. The transition state **10−5** transforms complex **10** into *ZEE*-diazidyldiazene with a "barrier" of −4 kcal/mol. **10−0** is the transition state for dissociation into $N_2 + 2N_3^{\bullet}$. The Gibbs free energy of activation is −13 kcal/mol, although, on the basis of the experiences with homolytic bond dissociation in diazidyldiazenes, this value may be too low. The reaction of **10** to **11** has a barrier of 3 kcal/mol. The fact that the CCSD(T) electronic energies fall from **99**, **10−10′**, or **10−11** over **10** to **10−5** suggests that there is no stationary point similar to **10** on the CCSD(T) hypersurface and that the reaction path from **99** will end either at **5** or at $N_2 + 2N_3^{\bullet}$.

Complex **99** presumably is a point on the symmetric approach path of N_3^- and N_5^+ with a free energy of 51 kcal/mol, relative to **3**. It has two imaginary frequencies, leading to **10−10′** and **10**. **10−10′** is a transition state for the transfer of the azidyl group from N2 to N4. This rearrangement is essentially a rotation of the azidyl group around the N6−N3 axis with a barrier of 7 kcal/mol.

The situation for **11**, which might be formed by addition of N_3^- to the outside of the N2 atom in N_5^+, is similar to that of **10**. Conversion of **11** to **10** has a Gibbs free energy of activation of 2 kcal/mol. The transition state **11−6** converts the complex **11** to *ZEZ*-diazidyldiazene **6** without a significant barrier. Our best result for the barrier is −0.1 kcal/mol, but because the B3LYP and MBPT(2) structures differ significantly, there is some doubt about the accuracy of this value. Like **10**, **11a** may also dissociate into $N_2 + 2\ N_3^{\bullet}$. The Gibbs free energy of activation at the B3LYP transition state (**11−0**) is lower than −17 kcal/mol. Because the CCSD(T) electronic energies fall from **10−11** over **11a** to **11−6** or **11−0**, the symmetric diazidylaminonitrene structure does not seem to be a minimum at the CCSD(T) level (Figure 6).

A comparison of the data in Table 13 shows that both B3LYP and MBPT(2) energies differ by as much as 17 kcal/mol from the CCSD(T) values. The CCSD values differ by up to 8 kcal/mol, often opposite to B3LYP.

The B3LYP bond lengths (Table 14a) vary significantly between the structures. All structures except **11a** can be seen as coupled N_5 and N_3 units. In **10,** the shape of the N_5 unit is similar to that of N1 to N5 in the diazidyldiazene **4**, except that the N1−N2 distance is nearly as short as the N4−N5 distance. The N2−N6 distance is so big that the distances in the N6 to N8 azidyl group are intermediate between H_3C-N_3 and $N_3^{\bullet}$. This is true for **10−10′** and **99**, too, but the N_5 unit is symmetric with bond lengths slightly bigger than in N_5^+. The averaged bond lengths in **10** are nearly identical to their counterparts in **10−10′**. The only exception is the N6−N2 distance, because of the different coordination mode (Table 15).

In the transition state **10−11**, the N2−N3 bond is elongated

TABLE 14: "Branched" N_8 Molecules

(A) Bond Lengths in Å at B3LYP/aug-cc-pVDZ

	8−7	7−6	6−2	1−2	2−3	3−4	4−5	1−8
10	1.158	1.211	1.981	1.150	1.402	1.271	1.128	
11a	1.138	1.248	1.572	1.156	1.572	1.248	1.138	
10−5	1.192	1.183	2.254	1.166	1.392	1.275	1.128	2.086
10−0	1.162	1.208	2.173	1.118	1.845	1.227	1.150	
10−11	1.144	1.237	1.702	1.148	1.539	1.251	1.139	
11−6	1.190	1.194	2.075	1.169	1.399	1.280	1.129	2.101
11−0	1.161	1.216	2.042	1.116	2.042	1.216	1.161	
10−10′	1.157	1.219	2.149	1.136	1.336	1.336	1.136	
99	1.160	1.207	2.144	1.134	1.326	1.326	1.134	

(B) Bond Lengths in Å at MBPT(2)/aug-cc-pVDZ

	8−7	7−6	6−2	1−2	2−3	3−4	4−5	1−8
10	1.194	1.226	2.137	1.181	1.364	1.300	1.146	2.490
11b	1.194	1.224	2.099	1.177	1.379	1.306	1.150	2.474
10−11	1.196	1.222	2.116	1.165	1.437	1.282	1.153	2.463
11−6	1.230	1.181	2.416	1.202	1.406	1.298	1.153	1.921
99	1.195	1.228	2.033	1.176	1.327	1.327	1.176	2.033

because of the missing π interaction, whereas the N2−N6 bond is shortened. Consequentially, both azidyl groups are more similar than in **10**. In **11**, both azidyl groups are identical with N2−N3 and N2−N6 distances that are only slightly longer than the NN single bond in $N_2(CH_3)_4$. In **10−5** and **11−6**, the transition states to linear *ZEE*- and *ZEZ*-diazidyldiazene and the N2−N6 and N1−N8 distances are nearly identical, and the N6 to N8 azidyl group is very similar to the N_3 radical. Transition states **10−0** and **11−0** have shapes very similar to **10** and **11**. Only bond lengths and angles involving the breaking bonds vary. The already weak N2−N6 and N2−N3 bonds have lengthened considerably, whereas the other bonds are distinctly more similar to those in N_2 and $N_3^{\bullet}$.

A comparison of MBPT(2) and B3LYP geometries shows that the complexes are less tightly bound at the MBPT(2) level. Complex **10** is a bit more similar to noninteracting N_5 and N_3 units, and **11b** has only C_S symmetry with a N2−N6 distance similar to **10**.

The electronic structures of the complexes, described in terms of NLMOs (see the Supporting Information), show distorted N_5 and N_3 units. The N_5 units show N2−N3 and N3−N4 single bonds and N1−N2 and N4−N5 triple bonds. However, in contrast to the usual pattern, the N1−N2 π bond with the lobes in the N1−N2−N3 plane is polarized toward the terminal atom. In **10−10′** and **99**, the equivalent N4−N5 π bond is polarized to the terminal atom, too. This is due to the interaction of N2 (and N4 in **10−10′** and **99**) with the loosely bound azidyl group.

In the C_{2v} structure **11a**, there are the usual triple and single bonds of the azidyl groups, two single bonds between them and N2 and an N1−N2 double bond. N1, N3, and N6 have two lone pairs, whereas N5 and N8 have one. The π lone pair at N1 is interacting strongly with the N2−N3 and N2−N6 σ antibonds.

The partial charges (Table 16) show a general pattern of negatively charged N_3 and positively charged N_5 units. The magnitude of the partial charge decreases with the distance between units from 0.46 in **99** to 0.0 in **11**. This can be interpreted as a tendency to go from N_5−N_3 to N_5^+ and N_3^- with the initial increase of distance.

The overlap-weighted NAO bond orders (see the Supporting Information) show weak N2−N6 bonds. They are weaker than the reference *trans*-$(H_3C)_2N-N(CH_3)_2$ for every structure. The N1−N2 bonds are stronger than that in *trans*-$H_3C-N{=}N-CH_3$,

TABLE 15: "Branched" N_8 Molecules

(A) Bond Angles in Degrees at B3LYP/aug-cc-pVDZ

	8−7−6	7−6−2	6−2−1	6−2−3	1−2−3	2−3−4	3−4−5
10	168.2	91.6	121.2	107.8	131.0	111.9	167.5
11a	178.6	106.1	131.7	96.7	131.7	106.1	178.6
10−5	158.8	78.9	110.1	121.8	128.1	109.9	169.6
10−0	177.3	90.5	126.4	107.3	126.3	104.2	178.6
10−11	176.9	103.0	129.6	99.5	130.7	107.5	173.6
11−6	153.5	84.0	113.5	112.4	134.1	110.7	170.8
11−0	179.1	100.0	132.4	95.2	132.4	100.0	179.1
10−10′	178.4	109.8	123.3	93.7	142.8	110.2	142.8
99	180.0	148.5	124.6	90.8	144.6	115.4	144.6

(B) Bond Angles in Degrees at MBPT(2)/aug-cc-pVDZ

	8−7−6	7−6−2	6−2−1	6−2−3	1−2−3	2−3−4	3−4−5
10	166.9	82.7	118.3	107.4	134.3	108.5	166.9
11b	166.2	82.9	119.5	99.6	141.0	107.9	169.4
10−11	165.7	82.8	119.0	103.3	137.6	106.5	171.1
11−6	164.2	-	-	-	124.5	110.2	170.1
99	180.0	147.1	126.4	90.9	142.7	112.5	142.7

TABLE 16: "Branched" N_8 Molecules, Natural Charges at B3LYP/aug-cc-pVDZ

	N8	N7	N6	N1	N2	N3	N4	N5
10	−0.10	0.17	−0.36	0.03	0.09	−0.18	0.24	0.12
11a	0.03	0.21	−0.24	−0.10	0.10	−0.24	0.21	0.03
10−11	−0.01	0.19	−0.28	−0.02	0.09	−0.20	0.20	0.03
10−5	−0.17	0.15	−0.22	0.05	0.01	−0.18	0.24	0.12
10−0	−0.06	0.13	−0.21	0.07	0.02	−0.16	0.17	0.04
11−6	−0.18	0.13	−0.14	−0.01	0.04	−0.18	0.22	0.10
11−0	−0.03	0.13	−0.14	0.04	0.03	−0.14	0.13	−0.03
10−10′	−0.13	0.16	−0.42	0.11	0.17	−0.18	0.17	0.11
99	−0.16	0.19	−0.49	0.11	0.20	−0.17	0.20	0.11

whereas the azidyl groups show bond orders between those of H_3C-N_3 and N_3^-.

Summary and Conclusions

We investigated possible products of the end-on addition of N_3^- to N_5^+ and searched for transition states to assess their stability. We optimized geometries at the B3LYP/aug-cc-pVDZ and MBPT(2)/aug-cc-pVDZ levels of theory. Single-point energies were calculated at CCSD(T)/aug-cc-pVDZ. To get data that are more relevant, we approximated enthalpies and Gibbs free energies at room temperature and 1 bar.

Analysis of the partial charges of N_5^+ and N_3^- as well as inspection of the lowest unoccupied orbitals of N_5^+ suggest that addition to the inside of the terminal nitrogen atoms is most likely. This would produce diazidyldiazenes. Other likely modes of attack are an approach of the azide anion along the C2 axis toward the inside of N3 (**99**) or a bidentate out-of-plane approach that connects N6 to N1 and N8 to N5. The former may lead to neutralization and fragmentation, whereas the latter mode of attack might lead to octazole or octaazapentalene.

We found several minimum structures that possibly arise from end-on addition of N_3^- to N_5^+. Lowest in energy are the chain structures, arising from bond formation between the terminal atoms of N_3^- and N_5^+. Lowest in Gibbs free energy is *EZE*[6]-diazidyldiazene (**7**), 13 kcal/mol higher than azidylpentazole, the currently accepted global minimum of the N_8 hypersurface. Although the *ZZE* rotamer **8** is a (shallow) minimum at lower levels of theory, CCSD(T) single-point calculations indicate that this structure is a transition state. The three rotamers of *E*-diazidyldiazene (**4**, **5**, and **6**) have Gibbs free energies 14−17 kcal/mol higher than azidylpentazole. Conversion of **4** to **5** has a barrier of ∼6 kcal/mol and we believe the transition state

between **5** and **6** to be of similar height. *E*- and *Z*-diazidyldiazenes are not connected by inversion of the N2−N1−N6 angle. The molecule dissociates before the angle reaches 180°. On the basis of chemical intuition, we believe that **4** is more likely to be formed than **7**.

The diazidyldiazenes are composed of two azidyl groups attached to the central diazene unit. The single bonds connecting these groups are weakest by the criteria of bond length, force constants, and overlap weighted NAO bond orders. Simultaneously breaking these bonds has barriers of 18 and 15 kcal/mol for **4** and **7**, respectively. Breaking the stronger inner bond of one azidyl group is as easy. The calculated barrier for dissociation into N_2 and N_6 is 19 kcal/mol for **4** and 16 kcal/mol for **7**. Unfortunately, we cannot expect to isolate any N_6, because the free energy of reaction, ~ -80 kcal/mol, is much larger than the barrier toward dissociation of N_6 into $3N_2$ (25−30 kcal/mol[19]).

Addition of N_3^- to one of the next-to-terminal atoms of N_5^+ does not result in stable structures. Although there are two minima (**10** and **11a**/**11b**) at B3LYP and MBPT(2), the CCSD(T) electronic energies and Gibbs free energies of the transition states toward lower energy structures are lower than those of **10** or **11**. Any molecule with a structure like **10** or **11** will immediately react to $N_2 + 2\ N_3^\bullet$ or (maybe) diazidyldiazenes.

In the gas-phase or in nonpolar solvents, addition of N_3^- to N_5^+ might produce diazidyldiazenes. These are sufficiently stable to be isolated at low temperatures, provided the Gibbs free energy of reaction can be dissipated before it destroys the molecule. Because the free energy of reaction is ∼150 kcal/mol in the gas phase, a reaction in solution is the only practical approach. In solution, the oppositely charged ions gain kinetic energy that is transferred to solvent molecules, which are pushed out of the way. A polar solvent will stabilize the reactants more than the product, further reducing the energy that needs to be dissipated.

Unfortunately, from the point of view of high energy density matter, a dissociation barrier of 19 kcal/mol is at least 10 kcal/mol lower than needed. Only in a solid-state structure, stabilized by a large lattice energy, is there any likelihood of stabilizing N_5^+ and N_3^- as an ion pair. Our gas phase calculations, though, suggest that transfer of an electron without covalent bond formation, most likely leads to dissociation of the N_5 unit. However, the top-on approach of N_3^- to N_5^+ might well lead to octazole or octa-azapentalene.[2a,c−e,3a,4] Another fascinating question analogous to $N_5^+ + N_3^-$ is a potential N_{10} species formed from N_5^+ and the pentazole anion,[21] N_5^-. Though the pentazole ring exists in organic species like phenyl-pentazole,[22] it is surprisingly unknown as an inorganic species lika NaN_5 or $Mg(N_5)_2$. However, extensive calculations support its existence as another potential HEDM candidate.[23]

Acknowledgment. This work was supported by the US Air Force Office of Scientific Research under Grant No. F49620-98-1-0477. S.F. wishes to thank Dr. Marcel Nooijen for valuable advice on using the DIP-STEOM-CCSD code.

Supporting Information Available: Vibrational frequencies of minima, natural localized molecular orbitals, overlap-weighted NAO bond orders, and absolute energies are presented. This material is available free of charge via the Internet at http://pubs.acs.org.

References and Notes

(1) Octaazacubane: (a) Lauderdale, W. J.; Stanton, J. F.; Bartlett, R. J. *J. Am. Chem. Soc.* **1992**, *96*, 1173−8. (b) Leininger, M. L.; van Huis, T. J.; Schaefer, H. F., III *J. Phys. Chem. A* **1997**, *101*, 4460−4. (c) Chen, C.; Shyu, S.-F. *Int. J. Quantum Chem.* **1999**, *73*, 349−56. (d) Engelke, R. *J. Am. Chem. Soc.* **1993**, *115*, 2961−7. (e) Engelke, R. *J. Org. Chem.* **1992**, *57*, 4841−6. (f) Trinquier, G.; Malrieu, J.-P.; Daudey, J.-P. *Chem. Phys. Lett.* **1981**, *80*, 552−7. (g) Alkorta, I.; Elguerro, J.; Rozas, I.; Balaban, A. T. *J. Mol. Struct. (THEOCHEM)* **1990**, *206*, 67−75.

(2) Octaazacubane and other minima: (a) Leininger, M. L.; Sherill, C. D.; Schaefer, H. F., III *J. Phys. Chem.* **1995**, *99*, 2324−8. (b) Tian, A.; Ding, F.; Zhang, L.; Xie, Y.; Schaefer, H. F., III *J. Phys. Chem. A* **1997**, *101*, 1946−50. (c) Gagliardi, L.; Evangelisti, S.; Roos, B. O.; Widmark, P.-O. *J. Mol. Struct. (THEOCHEM)* **1998**, *428*, 1−8. (d) Glukhovtsev, M. N.; Jiao, H.; Schleyer, P. v. R. *Inorg. Chem.* **1996**, *35*, 7124−33. (e) Ghimarc, B. M.; Zhao, M. *Inorg. Chem.* **1996**, *35*, 3289−97.

(3) Rearrangements of octaazacubane: (a) Gagliardi, L.; Evangelisti, S.; Widmark, P.-O.; Roos, B. O. *Theor. Chem. Acc.* **1997**, *97*, 136−42, (b) Evangelisti, S.; Gagliardi, L. *Il Nuovo Cimento D* **1996**, *18*, 1395−405. (c) Engelke, R.; Stine, J. R. *J. Phys. Chem.* **1990**, *94*, 5689−94.

(4) Rearrangements of other N_8 molecules: (a) Nguyen, M. T.; Ha, T. K. *Chem. Ber.* **1996**, *129*, 1157−9. (b) Chung, G.; Schmidt, M. W.; Gordon, M. S. *J. Phys. Chem. A* **2000**, *104*, 5647−50.

(5) Christe, K. O.; Wilson, W. W.; Sheehy, J. A.; Boatz, J. A. *Angew. Chem.* **1999**, *38*, 2004−9.

(6) We use the *Z*/*E* notation, which is a generalization of the familiar cis/trans notation applied to double bonds, to describe the shape of the conformers. Both N−N bonds adjacent to the central double bond in diazidyldiazene show predominantly σ bonding, but π-delocalization effects usually keep these molecules planar. To stick with one type of description, we label these conformations as *Z* or *E*, too. Gauche conformations in nonplanar molecules are designated "*g*", whereas dihedral angles close to 90° are represented by "*p*".

(7) White, C. A.; Kong, J.; Maurice, D. R.; Adams, T. R.; Baker, J.; Challacombe, M.; Schwegler, E.; Dombroski, J. P.; Ochsenfeld, C.; Oumi, M.; Furlani, T. R.; Florian, J.; Adamson, R. D.; Nair, N.; Lee, A. M.; Ishikawa, N.; Graham, R. L.; Warshel, A.; Johnson, B. G.; Gill, P. M. W.; Head-Gordon, M. *Q-Chem*, version 1.2; Q.-Chem, Inc.: Pittsburgh, PA 1998.

(8) ACES II is a program product of the Quantum Theory Project, University of Florida. Authors: Stanton, J. F.; Gauss, J.; Watts, J. D.; Nooijen, M.; Oliphant, N.; Perera, S. A.; Szalay, P. G.; Lauderdale, W. J.; Kucharski, S. A.; Gwaltney, S. R.; Beck, S.; Balková, A.; Bernholdt, B. E.; Baeck, K. K.; Rozyczko, P.; Hober, C.; Bartlett, R. J. Integral packages included are VMOL (Almlöf, J.; Taylor, P. R.); VPROPS (Taylor, P. R.); ABACUS (Helgaker, T.; Jensen, H. J. A.; Jørgensen, P.; Olsen, J.; Taylor, P. R.).

(9) Nooijen, M.; Bartlett, R. J. *J. Chem. Phys.* **1997**, *107*, 6812.

(10) Dunning, T. H., Jr. *J. Chem. Phys.* **1989**, *90*, 1007. Kendall, R. A.; Dunning, T. H., Jr.; Harrison, R. J. *J. Chem. Phys.* **1992**, *96*, 6769.

(11) Tobita, M.; Bartlett, R. J. *J. Phys. Chem. A* **2001**, *105*, 4107.

(12) Becke, A. D. *J. Chem. Phys.* **1992**, *96*, 2155. Becke, A. D. *J. Chem. Phys.* **1993**, *98*, 5648. Lee, C.; Yang, W.; Parr, R. G. *Phys. Rev. B* **1998**, *37*, 785.

(13) We are aware of the fact that reactions involving homolytic bond breaking can require multireference methods for an accurate description. We nevertheless chose to search all transition states with B3LYP, because previous experience indicates that it works.

(14) Glendening, E. D.; Badenhoop, J. K.; Reed, A. E.; Carpenter, J. E.; Weinhold, F. *NBO 4.0*.; Theoretical Chemistry Institute: University of Wisconsin, Madison, WI, 1996.

(15) Thermodynamic data are calculated based on statistical thermodynamics. STTHRM uses the rigid rotor, harmonic oscillator, and ideal gas approximations. Effects of nuclear spin on the rotational symmetry factor are ignored. Internal rotations are treated as vibrations. The electronic partition function is assumed unity. The program is available upon request from the RJB group.

(16) We abstain from using the name azidopentazole, used in previous publications, because the azidyl group is formally uncharged and the partial atomic charges sum up to only 0.14.

(17) Kucharski, S. A.; Watts, J. D.; Bartlett, R. J. *Chem. Phys. Lett.* **1999**, *302*, 295.

(18) Overlap-weighted NAO bond orders of reference molecules: $D_{\infty h}$ N_2 (1.88), C_S Me−N_3 (1.28, 1.64), C_{2h} Me−N═N−Me (1.29), C_{2h} Me_2N−NMe_2 (0.76).

(19) Gagliardi, L.; Evangelisti, S.; Barone, V.; Roos, B. O. *Chem. Phys. Lett.* **2000**, *320*, 518.

(20) Illenberger, E.; Comita, P.; Braumann, J. I.; Fenzlaff, H.-P.; Heni, M.; Heinrich, N.; Koch, W.; Frenking, G. *Ber. Bunsen-Ges. Phys. Chem.* **1985**, *89*, 1026.

(21) Ferris, K. F.; Bartlett, R. J. *J. Am. Chem. Soc.* **1992**, *114*, 8302. Perera, S. A.; Bartlett, R. J. *Chem. Phys. Lett.* **1999**, *314*, 381−7.

(22) Huisgen, R.; Ugi, I. *Chem. Ber.* **1957**, *90*, 2914. Wallis, J. D.; Dunitz, J. D. *J. Chem. Soc., Chem. Commun.* **1983**, *16*, 910−1.

(23) Bartlett, R. J. *Chem. Ind.-London* **2000**, *4*, 140−3. Structures and energies of polynitrogen and N_xH_y molecules and their spectroscopic characteristics: http://www.qtp.ufl.edu/∼bartlett/polynitrogen.doc.gz and http://www.qtp.ufl.edu/∼bartlett/hydrazine.doc.gz.